molecular pharmaceutics

Article

pubs.acs.org/molecularpharmaceutics

The Natural Cell-Penetrating Peptide Crotamine Targets Tumor Tissue *in Vivo* and Triggers a Lethal Calcium-Dependent Pathway in Cultured Cells

Fabio D. Nascimento,[†,‡] Lucie Sancey,[‡,§,∥] Alexandre Pereira,[⊥] Claire Rome,[§,∥] Vitor Oliveira,[#] Eduardo B. Oliveira,[▽] Helena B. Nader,[○] Tetsuo Yamane,[◆] Irina Kerkis,[⊥] Ivarne L. S. Tersariol,[¶] Jean-Luc Coll,*[,§,∥] and Mirian A. F. Hayashi*[,+]

[†]Grupo de Estudos em Odontologia, Universidade Bandeirante de São Paulo (UNIBAN), São Paulo, SP, Brazil

[§]INSERM U823, Institut Albert Bonniot, Grenoble, France

[∥]University Joseph Fourier, Grenoble, France

[⊥]Laboratório de Genética, Instituto Butantan, São Paulo, SP, Brasil

[#]Departamento de Biofísica, Universidade Federal de São Paulo (UNIFESP), São Paulo, Brazil

[▽]Departamento de Bioquímica e Imunologia, Universidade de São Paulo (USP), Ribeirão Preto, Brazil

[○]Departamento de Bioquímica, Universidade Federal de São Paulo (UNIFESP), São Paulo, Brazil

[◆]Laboratório de Bioquímica e Biologia Molecular, Centro de Biotecnologia da Amazônia (CBA), Manaus, AM, Brazil

[¶]Centro Interdisciplinar de Investigação Bioquímica (CIIB), Universidade de Mogi das Cruzes, Mogi das Cruzes, SP, Brazil

[+]Departamento de Farmacologia, Universidade Federal de São Paulo (UNIFESP), São Paulo, SP, Brazil

Supporting Information

ABSTRACT: Our goal was to demonstrate the *in vivo* tumor specific accumulation of crotamine, a natural peptide from the venom of the South American rattlesnake *Crotalus durissus terrificus*, which has been characterized by our group as a cell penetrating peptide with a high specificity for actively proliferating cells and with a concentration-dependent cytotoxic effect. Crotamine cytotoxicity has been shown to be dependent on the disruption of lysosomes and subsequent activation of intracellular proteases. In this work, we show that the cytotoxic effect of crotamine also involves rapid intracellular calcium release and loss of mitochondrial membrane potential as observed in real time by confocal microscopy. The intracellular calcium overload induced by crotamine was almost completely blocked by thapsigargin. Microfluorimetry assays confirmed the importance of internal organelles, such as lysosomes and the endoplasmic reticulum, as contributors for the intracellular calcium increase, as well as the extracellular medium. Finally, we demonstrate here that crotamine injected intraperitoneally can efficiently target remote subcutaneous tumors engrafted in nude mice, as demonstrated by a noninvasive optical imaging procedure that permits *in vivo* real-time monitoring of crotamine uptake into tumor tissue. Taken together, our data indicate that the cytotoxic peptide crotamine can be used potentially for a dual purpose: to target and detect growing tumor tissues and to selectively trigger tumor cell death.

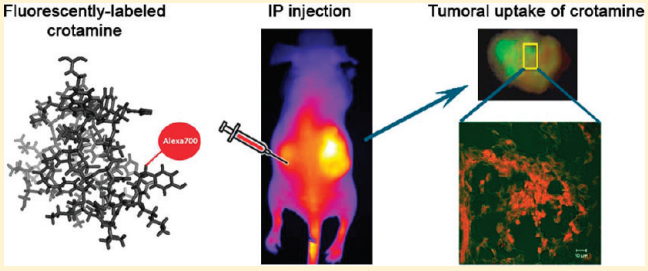

KEYWORDS: *mitochondria, cellular uptake, tumor-specific cell-penetrating peptides, actively proliferating cells, intracellular calcium*

INTRODUCTION

Molecular imaging and therapy for cancer would greatly benefit from specific targeting of contrast agents and therapeutic drugs to tumor tissues.[1] Currently, the main strategies are based on antibodies against surface markers or ligands for receptors and proteins preferentially expressed on the surface of cells in the target tissue.[2−4] Although antibodies can successfully target tumors,[5] their use is hindered by their bulky size[6] and by the genetic instability of tumor cells.[7] The payload ratio between the targeting device and its cargo can be amplified by incorporating the probe into polymers or nanoparticles.[8,9] Small specific ligands like RGD peptides are also being actively explored and will contribute to the definition of targeted delivery systems.[10,11] Moreover, low cell penetration ratios of anticancer drugs into tumors have been an important limiting

Received: February 3, 2011
Revised: October 17, 2011
Accepted: December 5, 2011
Published: December 5, 2011

factor for their efficacy, and the therapeutic index of many of these drugs could be improved by the coadministration of tumor-penetrating peptides such as disulfide-based cyclic RGD peptide (iRGD).[12]

Cell penetrating peptides (CPPs) can transport drugs into mammalian cells without requiring specific receptors. The first CPPs described were the Tat protein from HIV-1 and the Antennapedia homeobox protein; several small multicationic oligomers, such as polyarginines and polylysines, have since been described as CPPs.[13−15] CPPs can also mediate the delivery of therapeutic molecules *in vitro* and *in vivo*, providing an additional advantage for theranostic applications.[16,17] However, several biological features limit their usefulness in living animals,[18] many of which have been overcome by the development of activatable cell penetrating peptides (ACPPs),[19,20]whereby a covalently linked polyanionic domain minimizes the uptake by nontargeted cells. Interestingly, our group described that crotamine, a highly basic toxin of the South American rattlesnake *Crotalus durissus terrificus* venom, behaves as a CPP displaying a natural high specificity for actively proliferating cells.[21] Further studies on the mechanisms of crotamine internalization indicated that heparan sulfate proteoglycans present on the cell surface are required for the translocation of either crotamine alone or complexed with noncovalently bound cargoes.[22] Recently, we have shown that crotamine is internalized preferentially by highly proliferating cells, an event that induces cell death in a dose-dependent manner.[21,22] This cytotoxicity depends on the disruption of lysosomal vesicles and subsequent leakage of their contents into the cytosol, suggesting for the first time that lysosomes are the primary intracellular targets of crotamine.[23] In order to better understand this cytotoxicity, we studied the effect of crotamine on intracellular calcium dynamics, since calcium mobilization has long been implicated in cell injury.[24,25] We show that crotamine induces mitochondrial repolarization and an intracellular calcium overload, which is blocked by several inhibitors acting on the intracellular calcium mobilization pathway. Finally, we also demonstrated that crotamine targets tumor cells in living mice. The colocalization of fluorescent crotamine with tumor cells suggests crotamine as a potential marker of proliferating tumor cells *in vivo* and a candidate for specific targeting and delivery of drugs or therapeutic genes into proliferating cells.

MATERIAL AND METHODS

Culture reagents were purchased from Invitrogen (Carlsbad, CA, USA). All drugs and inhibitors were from Sigma Chemical Co. (St. Louis, MO, USA), or as specified in the text. Pep-1 was a kind gift from Dr. G. Divita (Centre de Recherches de Biochimie Macromoléculaire, UPR-1086 CNRS, 1919 Route de Mende, 34293 Montpellier, Cedex 5, France). Maurocalcine was purchased from Smartox (#07MAU001, Grenoble, France).

Purification of Crotamine. *Crotalus durissus terrificus* venom was extracted from snakes maintained at the serpentarium of the Faculdade de Medicina de Ribeirão Preto (FMRP), São Paulo University, and dried under vacuum. Six hundred milligrams of crude venom was dissolved in 5 mL of 0.25 M ammonium formate buffer pH 3.5, and the bulk of crotoxin, the major venom component, was eliminated by slow speed centrifugation as a heavy precipitate that formed upon slow addition of 20 mL of cold water to the solution. Tris base (1 M) was then added dropwise to the supernatant to raise the pH to 8.8. The solution was applied to a CM-Sepharose FF column (1.5 × 4.5 cm; Amersham Life Science, Buckinghamshire, U.K.) equilibrated with equilibrating solution [0.04 M Tris-HC1 buffer, pH 8.8, containing 0.064 M NaCl]. After the column was washed with 100 mL of equilibrating solution, crotamine [YKQCHKKGGHCFPKEKICLPPSSDFGKMDC-RWRWKCCKKGSG] was recovered as a narrow protein peak by raising to 0.64 M the concentration of the NaCl in eluting solution. The material was thoroughly dialyzed against water (benzoylated membrane, 3,000 Da cutoff) and lyophilized. Amino acid analysis after acid hydrolysis of a sample (4 N $MeSO_3H$ + 0.1% tryptamine; 24 h at 115 °C) indicated an overall yield of 72 mg (14.7 μmol) of crotamine and trace amounts of Thr, Ala and Val (purity >98%).

Labeling of Crotamine with Fluorescent Dye. Fluorescent crotamine derivatives were prepared using the Fluorolink Cyanine 3 (Cy3)-reactive dye (GE Healthcare, Buckinghamshire, U.K.) or the Alexa-700 Fluor dye (Invitrogen, Carlsbad, CA, USA) following the instructions of the respective manufacturers. After labeling, the remaining free fluorescent dye was eliminated using a Centricon spin column with a 3,000 Da cutoff (Centricon 3 molecular weight cutoff concentrator, Amicon, Millipore Corp., Billerica, MA, USA). The degree of labeling was estimated by absorbance measurements as indicated by the dye manufacturers and was confirmed by matrix-assisted laser desorption ionization time-of-flight mass spectrometry analyses (TofSpec-E, Micromass, U.K.).

Cell Culture. Mice melanoma B16F10 and HEK293(β_3)[26] cells were cultured in DMEM containing 10% fetal bovine serum (FBS), 50 units/mL penicillin, and 50 μg/mL streptomycin. Mice mammary carcinoma cells TS/A-pc and the subclone TS/A-pc-pGL3[26] were cultured in RPMI 1640 supplemented with 1% glutamine, 10% FBS, 50 units/mL penicillin, and 50 μg/mL streptomycin. TS/A-pc-pGL3 cells contain a luciferase vector and are therefore bioluminescent in the presence of luciferin. Wild type Chinese hamster ovary cells, CHO-K1, were cultured in F-12 medium containing 10% FBS, 50 units/mL penicillin, and 50 μg/mL streptomycin. Cell lines were cultured at 37 °C in a humidified 95% air and 5% CO_2 atmosphere for B16F10, TS/A-pc and TS/A-pc-pGL3, or a 2.5% CO_2 atmosphere for CHO-K1.

Cell Viability Assay. *MTT Assay.* Cell viability after exposure to crotamine was examined using the MTT assay, in which metabolically active mitochondrial dehydrogenase activity converts the tetrazolium salt 3-[4,5-dimethylthiazol-2-yl]-2,5-diphenyltetrazolium bromide (MTT; Sigma Chemical Co., St. Louis, MO, USA) to insoluble purple formazan crystals at a rate proportional to cell viability. Cultured B16F10 cells were plated in 96-well microtiter plates at a density of 2×10^5 cells/mL. After overnight incubation, the medium was removed and the cells were incubated with 0 to 20 μM toxin in the presence of 100 μL of culture medium supplemented with 0, 1 or 10% FBS for 4 or 24 h, at 37 °C, in an atmosphere of 5% CO_2 in air. At the end of the incubation, 20 μL of MTT solution (5 mg/mL in PBS) was added to each well. After 4 h, 100 μL of 0.04 N HCl in isopropanol was added to each well and thoroughly mixed before the plate was read on a FlexStation3 microplate reader (Molecular Devices, Sunnyvale, CA, USA, www.moleculardevices.com), using a test wavelength of 570 nm and a reference wavelength of 620 nm. Percent cytotoxicity was calculated as 100 × (1 − [optical density at 570−620 nm with toxin]/[optical density at 570−620 nm without toxin]). Two other CPPs, Pep-1[27] and maurocalcin,[28] were also examined on B16F10 cells in the presence of 1% or 10% FBS

at 1, 5, and 10 μM over 4 and 24 h, as described above. Results are expressed as mean values ± standard deviation (SD) of three independent experiments.

Determination of Cell Membrane Integrity Using a Fluorescence Assay. The membrane-permeable dye calcein-AM (Invitrogen) was used essentially as previously described.[29] CHO-K1 cells were washed twice with PBS, resuspended at 10^6/mL, and loaded with calcein-AM (Invitrogen) at a final concentration of 5 μM for 2 h at room temperature. Cells were washed four times to remove unincorporated dye, and 100 μL of cells (10^5 cells) was transferred to a quartz microplate for analysis. Crotamine (25, 50, or 100 μM) was then added to the calcein-loaded cells, and the fluorescence intensity of the crotamine-induced calcein release (I_r) was recorded after 10 min at excitation and emission wavelengths of 485 and 530 nm, respectively, in a FlexStation3 microplate reader. Fluorescence intensity corresponding to 100% of the potentially available internal calcein (I_{int}) was determined by treating the cells with 0.1% saponin for 10 min. The total fluorescence intensity of the cell population was assumed to be equivalent to the total potentially available intracellular calcein (I_{int}). The background fluorescence intensity (I_{bkg}) was determined by measuring the amount of calcein released from loaded cells without crotamine treatment over 10 min. Calcein efflux was calculated as the percent of fluorescence released = $[(I_r - I_{bkg})/(I_{int} - I_{bkg})] \times 100$.

Annexin V–FITC/PI Double Staining and Flow Cytometry Analysis. After treatment with 20 μM crotamine for 4 h, CHO-K1 cells were harvested, washed with cold medium supplemented with 10% FBS and suspended in binding buffer (0.01 M Hepes pH 7.4, 0.14 M NaCl and 2.5 mM $CaCl_2$) at a concentration of 1×10^6 cells/mL. The suspensions were transferred to tubes, and annexin V–FITC and propidium iodide (PI) were added according to the manufacturer's instructions (Becton Dickinson, Franklin Lakes, NJ, USA). Flow cytometry analysis was performed in a FACSCalibur cytometer (Becton Dickinson, Franklin Lakes, NJ, USA), using the CellQuest software (10,000 events were collected per sample). Control cells were treated with medium only. Results are presented as the mean ± SD of the triplicates, and the apoptosis rate was calculated as the percentage of cell death in comparison with the control.

Mitochondrial Potential. Mitochondrial activity was determined using the mitochondria potential sensor JC-1 (#T3168; Invitrogen, Carlsbad, CA, USA). B16F10 cells were cultured as described in 4-well Lab-Tek plates (Electron Microscopy Sciences, Hatfield, PA, USA) at a concentration of 5×10^4 cells/well and maintained at 37 °C in a 5% CO_2 incubator. JC-1 was then used as described by the manufacturer: 10 μg/mL for 10 to 20 min at 37 °C. Functional mitochondria were observed from 565 to 615 nm after excitation at 543 nm (in red), whereas dead mitochondria were observed from 500 to 550 nm after excitation at 488 nm (in green). Pictures were taken before and after addition of 1 μM crotamine or 1 μM staurosporine using an inverted LSM 510 confocal microscope (Carl Zeiss, Jena, Germany) equipped with a 40.0 × 1.25 numerical aperture (NA) oil immersion objective. The laser was set to the lowest power (>5%) that was able to produce a fluorescent signal. A pinhole of 1 airy unit was used. Images were acquired at a resolution of 512 × 512. Three-dimensional topographies were determined using the Topo application of the LSM 510 software (Carl Zeiss), and fluorescence intensities were quantified with the threshold application of the ImageJ software (http://imagej.nih.gov/ij/).

For quantitative analysis, at least 10 regions of interest (ROIs) were selected to quantify changes at 488 and 543 nm. All ROIs comprised cells chosen by the criteria of well-defined cellular limits, clear identification of the nucleus, and absence of intersection with neighboring cells. The size, number of pixels, and ratios between fluorescence intensity in the red (high membrane potential) and green (low membrane potential) channels in each ROI were calculated. Data are expressed as mean values of three independent experiments ± SD.

Ratiometric Ca^{2+} Imaging. Cells were loaded with Fluo-3 (#F-23915; Invitrogen) as described[30] and kept in the dark at room temperature until use. Approximately 5×10^4 B16F10 cells/well were plated on a 6-well plate with thin glass coverslips (0.1 mm) 24 h before the experiment. After the addition of 1 μM crotamine to the medium, ratiometric Ca^{2+} imaging was performed using an LSM 510 confocal microscope (Carl Zeiss). Images were acquired at 40-fold magnification and analyzed by LSM 510 Image Examiner software. The following configurations were used: objective, Plan-Neofluar 40×/1.3 NA oil; pinhole, 2.55 airy units; frame size, 1024 × 1024; scan speed, 11. The acquisition rate was adjusted to ∼14 ratios/min. Confocal Ca^{2+} images were obtained by off-line deconvolution (no-neighbor algorithm). The deconvoluted images were used to construct ratio images (340/380 nm) pixel by pixel. The calcium fluorescence dye Fluo-3 (503–553 nm) was excited with argon laser at 488 nm, and the green light was captured by a band-pass 500–550 nm filter. Differential interference contrast (DIC) images were obtained using a HeNe2 laser at 633 nm. For real-time microscopy, the image frame was continuously acquired every 4.27 s. Quantification of emitted fluorescence in the presence or absence of thapsigargin (1 μM) was calculated by taking the average fluorescence of each acquired image during the measurement.

Calcium Measurements by Microfluorimetry. Changes in $[Ca^{2+}]_i$ were determined by microfluorimetry using the FlexStation3 plate reader following the instructions of the manufacturer. Briefly, cells were seeded the night prior to the experiment at a density of 5×10^4 cells/well in 96-well black walled, clear-bottom microplates with 100 μL of cell culture medium per well. Cells were incubated for 60 min at 37 °C with the FlexStation Calcium Assay Kit (Molecular Devices Corp.) containing 2.5 mM probenecide in a final volume of 200 μL per well. Samples were excited at 485 nm, and fluorescence emission was read at 525 nm, every 1.52 s for 120 s, resulting in 79 readouts per well. Following 20 s of monitoring basal fluorescence intensity for $[Ca^{2+}]_i$ levels of nonstimulated cells, crotamine at a final concentration of 1 μM was applied to the cells, and induced $[Ca^{2+}]_i$ transients were monitored for up to 100 s. The response to agonist was determined as peak fluorescence minus basal fluorescence intensity using the SoftMaxPro software (Molecular Devices Corp.). Whenever used, the inhibitors nigericin (1 μM), A23187 (1 μM) and EGTA (5 mM) were preincubated with the cells for 5 min; thapsigargin (1 μM), NH_4Cl (1 mM) and ryanodine (2 μM) were preincubated for 30 min, and chloroquine (100 μM) was preincubated for 60 min. Data are expressed as mean values ± SD of at least five independent experiments.

***In Vivo* Crotamine Localization in Tumor Tissue.** *Tumor Engrafting.* To test the accumulation of crotamine–Alexa 700 in tumor tissues of living mice, tumors were engrafted into 6–8 week old female NMRI nude mice (Janvier, Le Genest-Saint-Isle, France) by two distinct routes of injection approximately 1–2 weeks before the experiment. In one case, murine B16F10

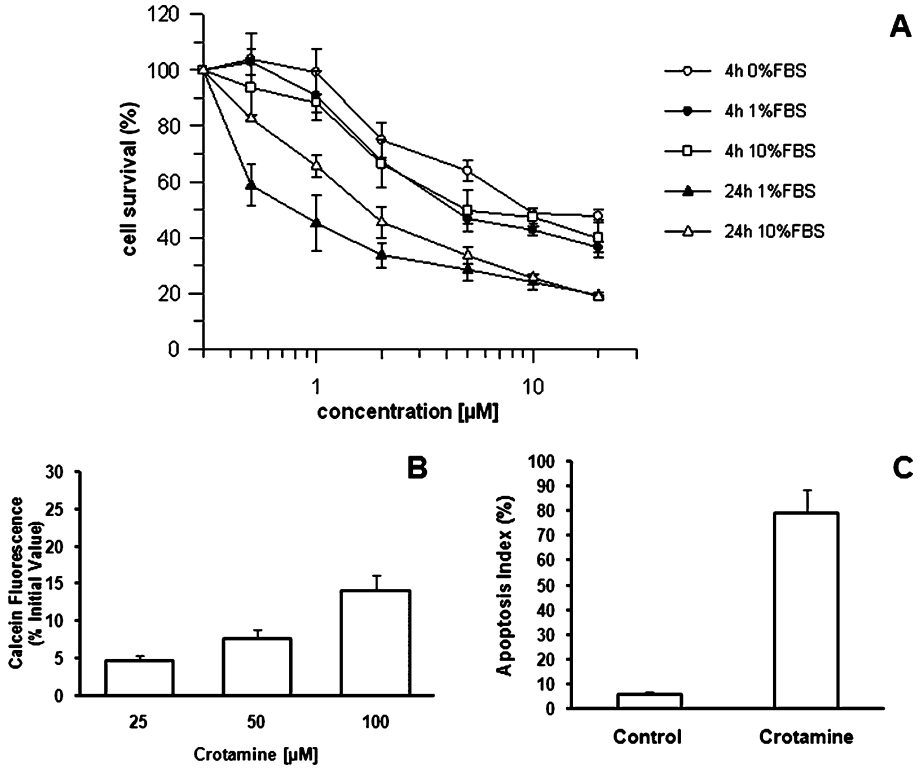

Figure 1. Cell viability assays. (A) B16F10 cells were incubated with 0, 0.5, 1, 2, 5, 10, and 20 μM crotamine for 4 and 24 h, and the cell survival rate was measured by the MTT assay. The percentage of cell growth in the control group was designated as 100%. (B) The calcein-AM assay for membrane integrity was performed by pretreating CHO-K1 cells with 25, 50, and 100 μM crotamine for 24 h before incubation with calcein-AM and cell lysates. The fluorescence intensity of calcein-AM present in the cytosol after each treatment is shown. Calcein efflux was calculated as percent fluorescence release = $[(I_r - I_{bkg})/(I_{int} - I_{bkg})] \times 100$. (C) After incubation with 20 μM crotamine for 4 h, CHO-K1 cells were labeled with annexin V–FITC and propidium iodide (PI). Apoptosis was evaluated by FACS analysis of the emitted fluorescence in both channels, green (FITC) and red (PI). The rate of apoptosis was calculated as the percentage of cell death compared to the control cells, which were treated only with medium. Results are expressed as mean values ± SD of three independent experiments.

or TS/A-pc cells (1×10^6 cells) were injected subcutaneously (SC) into the left or right hind limbs, respectively, 2 weeks before the experiment. In the other case, 5×10^5 TS/A-pc-pGL3 cells were injected SC or intraperitoneally (ip) approximately 7 days before the experiment. All animals were caged and handled ethically according to international rules of animal care, stated by the International Animal Welfare Recommendations, in accordance with the Guidelines for the Use of Animals in Biochemical Research,[31] and were approved by the regional Ethics Committee.

Fluorescence Reflectance Imaging (2D-FRI). Fluorescence reflectance imaging was carried out in mice anesthetized with 3.5/4% isoflurane/oxygen for induction and 1.5/2% thereafter (CSP, Cournon, France). A crotamine–Alexa 700 solution (10 μg ≈ 2 nmol in 100 μL/animal) was injected ip at the beginning of the experiment. Mice were illuminated with 660 nm light-emitting diodes equipped with interference filters, and both fluorescence images and black and white pictures were acquired by a back-thinned CCD camera at −80 °C (ORCAII-BT-512G, Hamamatsu, Massy, France)[10,26,32] fitted with a high-pass RG 9 filter (Schott, Clichy, France). At the end of the experiment, mice were euthanized and dissected to better visualize the colocalization of crotamine–Alexa 700 with the bioluminescent tumor cells in the tumor tissue.

Bioluminescence Imaging. Five minutes after ip injection of luciferin (150 μg/g; Promega, Charbonnières, France), mice were anesthetized, and both bioluminescence images and black and white pictures were acquired using a back-thinned CCD camera at −80 °C (ORCAIIBT-512G, Hamamatsu).

Microscopy Imaging. To assess the localization of crotamine in melanomas formed by SC injection of B16F10 cells, Cy3-conjugated crotamine was injected ip (10 μg/animal), 24 h before sacrifice. Frozen sections from excised melanoma were obtained using a cryomicrotome (model CM 1100, Leica, Germany) and were analyzed by LSM 510 confocal microscopy. Tissue sections (5–7 μm thick) prepared on a microtome from paraffin-embedded blocks of this same tumor tissue were mounted on adhesive microscope slides, and routine hematoxilin and eosin (HE) histological staining was used for examination by light microscopy.

Frozen sections were also obtained from tumors engrafted by ip injection of TS/A-pc-pGL3 cells and analyzed using fluorescence microscopy (Axiocam, Carl Zeiss, Jena, Germany) to observe the crotamine–Alexa 700 localization in slices of the tumor nodule.

RESULTS

***In Vitro* Evaluation of Crotamine Toxicity.** We have previously observed that crotamine is capable of penetrating specifically in proliferating cells and that its toxicity is concentration-dependent.[21,22] Using the MTT assay, we show here that about 50% of the B16F10 cells die within 4 h of treatment with 5–20 μM crotamine, while approximately 0.5–1 μM crotamine was enough to reach the IC_{50} after 24 h (Figure 1A). Moreover, at least for this cell line, the influence of the presence

dx.doi.org/10.1021/mp2000605 | *Mol. Pharmaceutics* 2012, 9, 211–221

of serum in the culture medium was less pronounced compared to our previous report showing that decreasing the concentration of serum negatively affects the cytotoxic effects of crotamine on CHO-K1 cells.[23] Importantly, two other well-known CPPs, Pep-1 and maurocalcine, were also evaluated in these cells. No toxicity was detected after incubation with up to 10 μM of each peptide for 4 and 24 h, suggesting that crotamine-mediated toxicity on tumoral cells is not a common property shared by natural or synthetic CPPs (Supporting Information S1).

The acetoxymethyl ester of calcein (calcein-AM) is a fluorescein derivative and nonfluorescent vital dye that passively crosses the cell membrane of viable cells. Calcein-AM is converted by cytosolic esterases into green fluorescent calcein that is retained by cells with intact membranes. The use of calcein-AM showed that, after treatment for 10 min with up to 100 μM crotamine, the cell membrane was mostly intact, with a maximum calcein efflux lower than 15% (Figure 1B). Furthermore, experiments using annexin V−FITC and propidium iodide (PI) confirmed that crotamine induces apoptosis (Figure 1C). Caspase activation was also confirmed here (Supporting Information S2), which is in line with our previous data.[23]

Mitochondria play a major role in active cell death. Quantification of the mitochondrial membrane potential was determined by measuring the cellular uptake of the fluorescent dye JC-1 after treatment with 1 μM crotamine. JC-1 is a cationic dye that exhibits potential-dependent accumulation in mitochondria, indicated by a fluorescence emission shift from green (500 to 550 nm) to red (565 to 615 nm). At low membrane potentials, JC-1 produces green fluorescence; at high membrane potentials, it forms "J-aggregates" with red fluorescence correlated with mitochondrial activity. Consequently, the loss of mitochondrial membrane potential is indicated by a decrease in the red/green fluorescence intensity ratio.[33] As shown in Figure 2, a significant loss of mitochondrial membrane potential was observed by comparative analysis of the fluorescence before (Figure 2A) and after (Figure 2B) addition of 1 μM crotamine, in the same way as that observed in the positive control experiment with 1 μM staurosporine (Figure 2C and Figure 2D, before and after treatment, respectively). Based on quantitative analyses of changes in the red and green channels of at least 10 selected regions of interest (ROIs), a fold-decrease of 3.35 ± 0.50 and 3.09 ± 0.22 of the red/green fluorescence (i.e., functional/dead mitochondria) ratio was observed after less than 10 min of exposure to crotamine and staurosporine, respectively (Figure 2E).

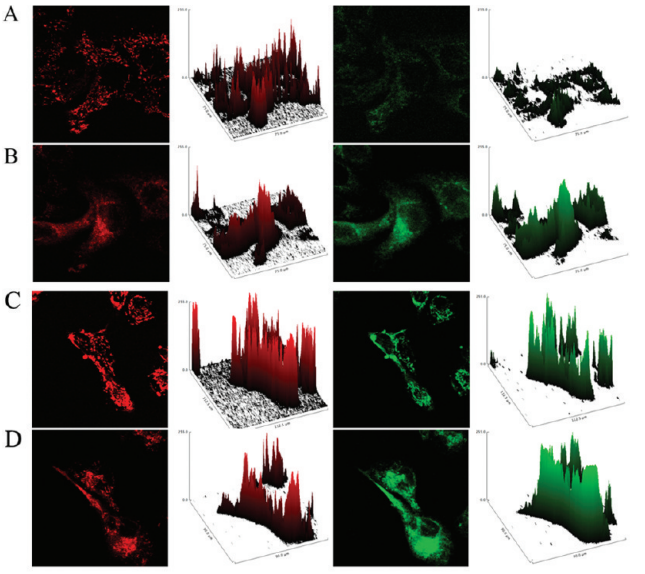

E

Treatment	Ratio before treatment	Ratio after treatment	Ratio (before/after)
Crotamine	3.71 ± 0.55	1.14 ± 0.14	3.35 ± 0.50 (p=0.019)
Staurosporine	2.14 ± 0.38	0.72 ± 0.22	3.09 ± 0.22 (p=0.015)

Figure 2. Mitochondrial potential determined by biphotonic fluorescence microscopy. Mitochondrial potential of B16F10 cells before (A, C) and after (B, D) treatment with 1 μM crotamine (A, B) or 1 μM staurosporine (C, D) evaluated with JC-1 dye. Mitochondrial polarization could be monitored by the red (functional) or green (repolarized) fluorescence. (E) Red/green ratios before and after treatment with crotamine and staurosporine. Here, we show a decrease in the red/green fluorescence intensity ratio of about 3.35-fold after crotamine treatment, while control experiment with staurosporine showed about 3.09-fold decrease. Results are expressed as means ± SD.

Intracellular Calcium Dynamics. A change in the permeability of the mitochondrial membrane is a critical step in apoptosis. It has been demonstrated that the trigger for apoptosis is spatially localized, initiating at one or a few mitochondria, preceding the loss of mitochondrial energetics and subsequent temporal propagation of a calcium-dependent mitochondrial membrane permeability.[34] We have evaluated crotamine-triggered intracellular calcium dynamics by real-time monitoring of free calcium (Ca^{2+}) release by confocal microscopy. Addition of 1 μM crotamine to cultured B16F10 cells pretreated with Fluo-3 fluorescent dye initiated a Ca^{2+} wave that could be detected by the increase of the green fluorescence inside the cell cytoplasm (Figure 3A). This change in free intracellular calcium concentration ($[Ca^{2+}]_i$) was estimated semiquantitatively by monitoring the intensity of the intracellular fluorescence (Figure 3B, green △). Interestingly, this Ca^{2+} wave could be almost completely blocked by pretreating cells with the sarco/endoplasmic reticulum Ca^{2+}-ATPase (SERCA) inhibitor thapsigargin (Figure 3B, red ○). Quantitative analysis shows a decrease of more than 97% of the emitted fluorescence mean based on Ca^{2+} release induced by crotamine in the presence of 1 μM thapsigargin (Figure 3C). Figure 3 shows representative photos revealing the kinetics of intracellular Ca^{2+} release in B16F10 cells, as observed by real-time confocal microscopy after addition of crotamine. The green fluorescence due to intracellular Ca^{2+} release of each snapshot from panel A was quantified by digital analysis, presented in panel B. The respective images showing the inhibition of Ca^{2+} wave by thapsigargin are presented in Supporting Information S3.

Characterization of the Crotamine-Induced Release of Intracellular Calcium. In order to better characterize crotamine-induced $[Ca^{2+}]_i$ transients, we employed a microfluorimetric assay using the FlexStation3 system. The effect of several pharmacological inhibitors acting on different steps of the intracellular signaling transduction mediated by Ca^{2+} oscillations was evaluated. We observed that crotamine-induced $[Ca^{2+}]_i$ transients require both the influx of extracellular Ca^{2+} and the release of Ca^{2+} from intracellular stores (Figure 4). The presence of either the extracellular Ca^{2+} chelator EGTA or the SERCA inhibitor thapsigargin, which depletes intracellular Ca^{2+} stores, led to an almost complete loss of the crotamine-induced $[Ca^{2+}]_i$ response. The contribution of lysosomes to the

dx.doi.org/10.1021/mp2000605 | Mol. Pharmaceutics 2012, 9, 211−221

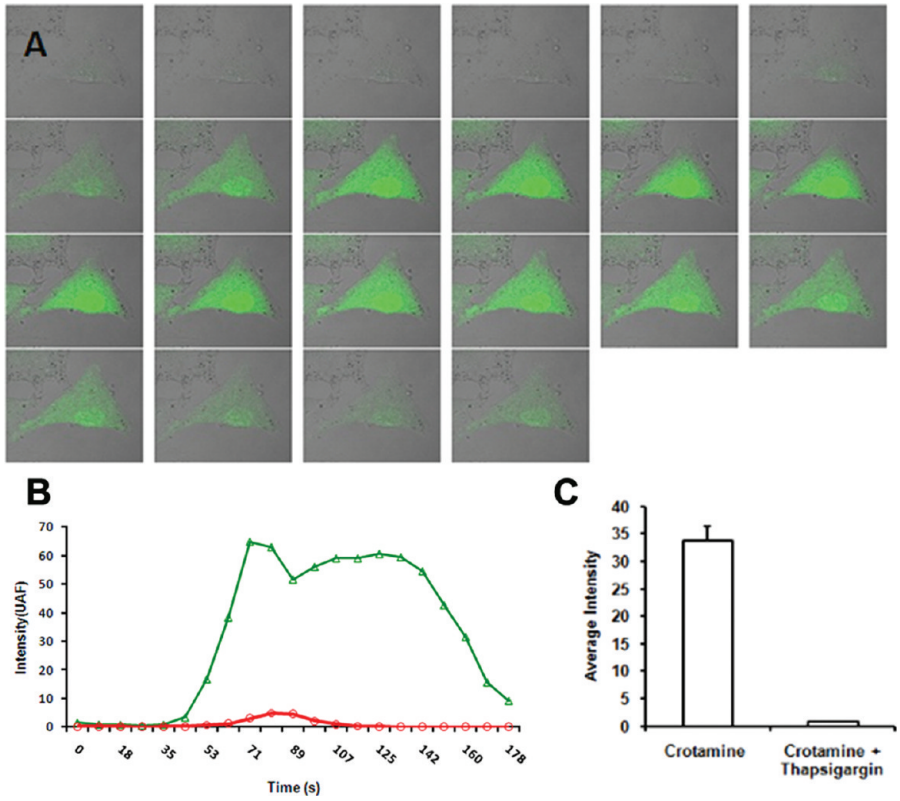

Figure 3. Effect of crotamine on calcium mobilization in B16F10 cells loaded with Fluo-3. (A) Sequential time course acquisition of intracellular calcium mobilization by ratiometric Ca^{2+} imaging of B16F10 cells loaded with Fluo-3. The time course image acquisitions were performed by confocal microscopy, after addition of 1 μM crotamine. (B) Quantitative cytosolic Ca^{2+} fluorescence ratios in B16F10 cells pretreated (red ○) or not (green △) with the SERCA inhibitor thapsigargin before the addition of crotamine. (C) Quantitative representation of fluorescence emission averages in both conditions.

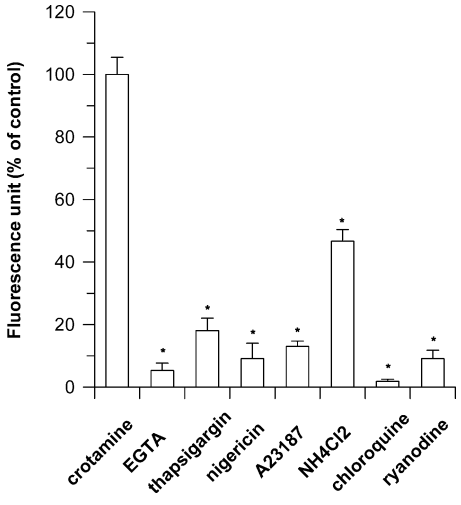

Figure 4. Evaluation of crotamine-induced $[Ca^{2+}]_i$ transients in B16F10 cells in the presence of inhibitors. Peak values of induced $[Ca^{2+}]_i$ levels obtained in the presence of 1 μM crotamine were considered 100% (control). After preincubation with several inhibitors of calcium-signal transduction pathways, the intracellular calcium concentration was evaluated as indicated. *$p > 0.05$ compared to crotamine control data obtained in the absence of inhibitors. Data are shown as mean values ± SD of at least five independent experiments.

crotamine-induced $[Ca^{2+}]_i$ transients was confirmed by the nearly complete block achieved by the K^+/H^+ uncoupler nigericin and the Ca^{2+} ionophore A23187. Nigericin, a monovalent cation ionophore, also induces intracellular alkalinization similarly to NH_4Cl, although this latter compound was much less effective in blocking the crotamine-induced $[Ca^{2+}]_i$ response. As expected, the lysosomotropic agent chloroquine was the most effective blocker, confirming the importance of lysosome targeting by crotamine. The inhibition of calcium-induced calcium release (CICR) mechanism by treatment with ryanodine, which blocks the calcium release mediated by ryanodine receptors (RyRs), also led to a significant effect on the crotamine-induced $[Ca^{2+}]_i$ transients (Figure 4).

This crotamine-induced $[Ca^{2+}]_i$ response might then lead to the activation of Ca^{2+}-activated hydrolyzing enzymes, such as the apoptosis promoter enzyme caspase, which was shown to be activated in tumor cells by crotamine (Supporting Information S2).[23]

***In Vivo* Crotamine Uptake into Tumors.** Noninvasive real-time optical imaging was used for tracking the specific localization of fluorescently labeled crotamine to tumors. We evaluated the accumulation of crotamine into B16F10 and TS/A-pc SC tumors after ip injection of crotamine–Alexa 700 (Figure 5). High crotamine uptake was observed macroscopically only in TS/A-pc tumors by 2D-FRI in both living animal and excised tumor tissue (Figures 5A and 5B). Unfortunately, fluorescent signal was not detectable in the highly pigmented B16F10 SC tumors, even in the excised tumor tissue, because of the pronounced absorbance of this tissue caused by the production of melanine by B16F10 cells. However, Cy3–crotamine fluorescence could be positively identified in these B16F10 cells in slices of the growing tumor tissue (Figure 5C). Moreover, HE staining sections confirmed the typical morphology of melanoma cells in this tissue (Figure 5D).

dx.doi.org/10.1021/mp2000605 | *Mol. Pharmaceutics* 2012, 9, 211–221

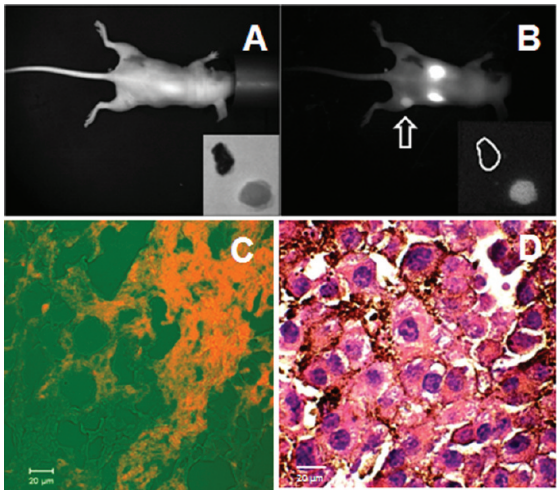

Figure 5. 2D-FRI imaging of tumor-bearing mice 75 min after Alexa 700−crotamine injection. NMRI nude mice were grafted SC with TS/A-pc cells (right hind limb) and B16F10 cells (left hind limb) and observed under white light (A) or after Alexa 700 excitation (B). Crotamine−Alexa 700 (10 μmol/100 μL/mouse) accumulated in the fluorescent TS/A-pc tumors (arrow in panel B), but was not visible in B16F10 tumors containing high levels of melanine (white outline in panel B). Cy3−crotamine had strong red fluorescence in melanoma cells in growing tumors (C), and HE stained sections show typical morphology of melanoma cells (D). (A) Black and white imaging and (B) 2D-FRI optical imaging of the same mouse. (C) Merged images obtained by differential interference contrast (DIC) and fluorescent confocal microscopy (Fm). Green is an artificial microscope color. Scale bars: (C, D) 20 μm.

Monitoring the time course of crotamine−Alexa 700 uptake into TS/A-pc SC tumors revealed the presence of a fluorescent signal as early as 15 min after ip injection, which lasted for more than 5 h (Figure 6). As shown in Figure 6, the best tumor-to-

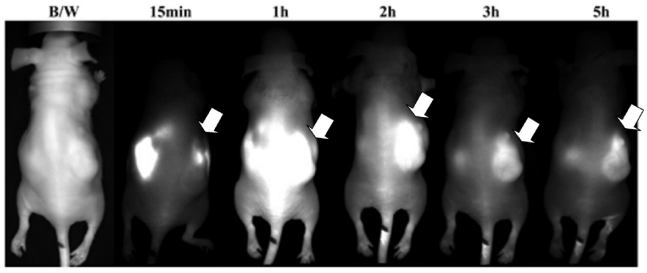

Figure 6. Time course of the uptake of ip-injected crotamine−Alexa 700 by SC injected murine breast TS/A-pc tumors in living animal. 2D-FRI optical imaging of TS/A-pc SC tumor-bearing mice was obtained from 15 min to 5 h after ip injection of fluorescent crotamine (10 μmol/100 μL/mouse), showing a major uptake of crotamine into the tumor (indicated by arrows). B/W: Black and white imaging of the mouse.

background fluorescence ratio was observed 3 h after crotamine−Alexa 700 injection. Real-time monitoring of ip injected crotamine−Alexa 700 in mice with SC tumors showed its nonspecific spread in the animal peritoneal cavity, followed by an immediate specific uptake into tumor nodule and a rapid renal clearance of crotamine (Supporting Information S4).

In order to further demonstrate the precise targeting of the tumor by crotamine, mice with tumors engrafted by ip injection of bioluminescent TS/A-pc-pGL3 cells were monitored after ip injection of crotamine−Alexa 700. Overlapping bioluminescence (green) and crotamine fluorescence (red) could be observed in all tumor tissues as soon as 15 min after crotamine injection (Figure 7 and Supporting Information S4) and lasted for at least 24 h (Supporting Information S5). In this model, the tumors develop as scattered nodules, forming a peritoneal carcinomatosis.[35] When crotamine−Alexa 700 was ip injected 3 h before optical imaging acquisition, several spots of colocalization were observed in the animals (Figure 7C,F,I). Bioluminescence and fluorescence analyses were carried out with animals lying on their sides (Figure 7A−C) or on their backs (Figure 7D−F). Finally, at the end of the experiments, animals were sacrificed and some organs were collected for bioluminescence and fluorescence analyses (Figure 7G−I). Dissected tumor nodules were also analyzed by 2D-FRI, and colocalization of crotamine and tumor nodules was observed (Figure 7J). The colocalization shown in yellow corresponds to the superposition of the green bioluminescent signal and the red fluorescent signal coming from crotamine−Alexa 700.

The biodistribution of radioactively labeled crotamine has been previously shown by others to be preferentially accumulated in kidneys of bare animals.[36] Using 2D-FRI to monitor the crotamine−Alexa 700 biodistribution, we also observed a high accumulation in kidney and a clear uptake of this molecule by the tumor nodule (Supporting Information S4 and Supporting Information S5). Note that crotamine is rapidly cleared from nonproliferating tissues.

These tumor nodules were also sliced, and a representative picture of 6−10 μm cryostat sections is presented. Preferential uptake of crotamine−Alexa 700 by the potentially proliferating cells localized at the peripheral region of the tumor mass was observed (Figure 8).

DISCUSSION

Two features of crotamine, its cytotoxicity and its affinity for actively proliferating cells,[21−23] led us to further investigate its potential applications against cancer. Selective penetration of crotamine into actively proliferating cells has been confirmed by 5-BrdU incorporation studies.[14] Once in proliferating cells, crotamine can be toxic in a concentration dependent manner, and we have suggested lysosomes as the primary target of this cytotoxicity.[23] However, organelles such as the endoplasmic reticulum (ER) and mitochondria play a major role in cell signaling pathways, cellular response to stress and cellular activation of apoptosis.[25,37−39] In addition, Ca^{2+} can trigger mitotic division or cell death in several cell types.[40] This toxic role of Ca^{2+} is associated with Ca^{2+}-activated hydrolyzing enzymes,[41] and both the Ca^{2+} release from the ER and the capacitive Ca^{2+} influx through Ca^{2+} release-activated Ca^{2+} channels have been proposed to be apoptogenic.[37] In addition, there is also solid evidence suggesting that a sudden change in the permeability of the mitochondrial membrane (mitochondrial permeability transition, MPT) plays a critical role in apoptosis, and it seems to participate in the propagation of Ca^{2+}-dependent intracellular events associated with cell death.[24] We therefore investigated the molecular mechanisms underlying the ER-mitochondria axis, focusing on Ca^{2+} as a potential mediator of crotamine-mediated cell death.

We first showed that B16F10 cells are highly sensitive to crotamine (Figure 1A), most probably due to the high proliferative features of this cell line. In fact, the presence of serum did not affect the viability of B16F10 cells, as much as previously observed for CHO-K1 cells after 24 h crotamine

dx.doi.org/10.1021/mp2000605 | Mol. Pharmaceutics 2012, 9, 211−221

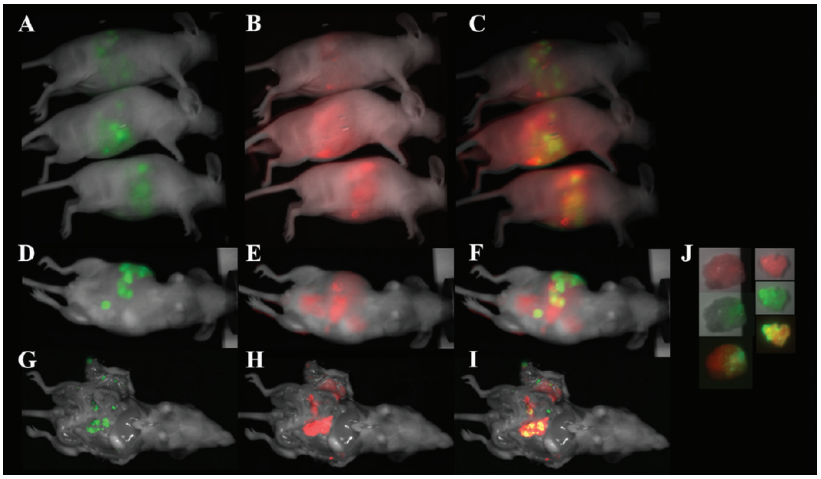

Figure 7. Optical imaging of ip TS/A-pc-pGL3 tumor-bearing mice showing a specific accumulation of crotamine in tumor tissues. Mice with ip TS/A-pc-pGL3 tumors were ip injected with 10 μmol crotamine−Alexa 700/mice (red, B, E, H) and luciferin (green, A, D, G) 3 h and 5 min before optical imaging, respectively. Co-localization (yellow, C, F, I) of bioluminescence and crotamine fluorescence in tumors could be observed in living animals lying on their sides (A−C) or lying on their backs (D−F), or after sacrifice and organ exposure (G−I), or in dissected tumors (J).

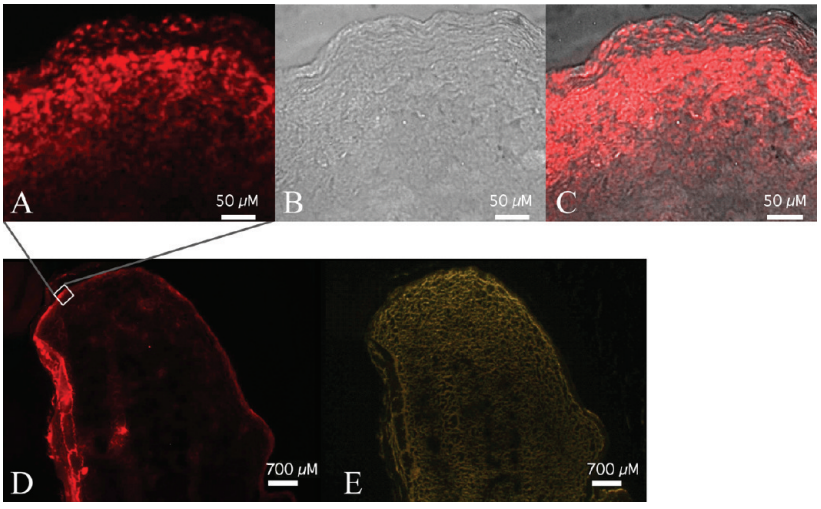

Figure 8. Fluorescence microscopy of tumors. Animals were sacrificed 3 h after crotamine injection. Following removal of TS/A-pc tumors, frozen slices of this tissue were analyzed under fluorescent microscopy. Fluorescent signal (red) was mainly observed in the tumor periphery cells; (A and D) fluorescent microscopy (Fm); (B and E) differential interference contrast (DIC); (C) merge of A and B. Scale bars: (A−C) 50 μm; (D, E) 700 μm.

treatment, in which a significant influence of serum on the maximum cell death percentage was shown .[23] Interestingly, the viability of B16F10 cells was not significantly affected by up to 10 μM of two other CPPs, synthetic Pep-1[27] and naturally occurring maurocalcine,[28] emphasizing that crotamine cytotoxicity is mediated by the peptide itself rather than by an unspecific effect caused by excessive amounts of peptide (Supporting Information S1). Along the same line, experiments using calcein-AM (Figure 1B) confirmed that the effect of crotamine was not due to disruption of plasma membranes. Moreover, experiments with annexin V−FITC and propidium iodide (PI) (Figure 1C) and the activation of hydrolyzing enzymes, namely, caspases (Supporting Information S2), confirmed that crotamine induces apoptosis.[23]

We also show here that as little as 1 μM crotamine is able to lose the mitochondrial membrane potential (Figure 2). In addition, 1 μM crotamine triggered a wave of intracellular calcium (Figure 3A) that was blocked by the SERCA inhibitor thapsigargin (Figure 3B,C), suggesting an important role for the ER in the modulation of cytosolic Ca^{2+}. We believe that the residual Ca^{2+} wave remaining after treatment with thapsigargin (Figure 3B and Supporting Information S3) could come from intracellular organelles. The influx of extracellular Ca^{2+} was also demonstrated by blocking the Ca^{2+} transients with the extracellular Ca^{2+} chelator EGTA. In the same way, the role of lysosomes in crotamine-induced Ca^{2+} transients was confirmed by the block induced by the K^+/H^+ uncoupler nigericin, the calcium ionophore A23187, and NH_4Cl; the participation of lysosomes was confirmed using the lysosomotropic agent chloroquine. The less pronounced block observed during NH_4Cl treatment might be due to the inhibition of the Ca^{2+} entry pathway previously described for this compound.[42] Finally, the inhibition of calcium-induced calcium release (CICR) by treatment with ryanodine significantly affected crotamine-induced Ca^{2+} transients (Figure 4).

It is notable that disrupting the pH gradient of acidic stores with alkalinizing agents such as bafilomycin A1, NH^{4+}, chloroquine, or nigericin leads to a block of lysosome

membrane fusion. Since the immediate consequence of intraluminal alkalinization is also luminal loss of Ca^{2+} from acidic endosomes and because Ca^{2+} plays a pivotal role in vesicle trafficking and fusion,[43] it can be extrapolated that luminal Ca^{2+} loss is a more direct cause of the inhibitory effect of the above agents on the fusion of endosomes, autophagosomes, amphisomes, and lysosomes.[44,45] Our data suggest that crotamine can mobilize Ca^{2+} from endosomal/lysosomal acidic stores. Also, we have previously shown that crotamine can induce lysosomal membrane permeabilization.[22,23] So, according to this scenario, pretreatment of cells with these alkalinizing agents, which deplete acidic Ca^{2+} stores by disrupting the pH gradient, blocked the crotamine-induced Ca^{2+} transient from acidic stores (Figure 4).[46] Taken together, our data strongly suggest that crotamine can mobilize Ca^{2+} from endosomal/lysosomal acidic stores.

It is worth mentioning that the membrane integrity of cells after treatment with crotamine was also evaluated using the calcein-AM assay for cell membrane integrity (Figure 1C), which ruled out a role of pore formation in the effect of crotamine on intracellular calcium waves.

Collectively, these observations suggest that the mechanism underlying the cytotoxicity of crotamine involves multiple targets because it interacts with lysosomes[22] to trigger intracellular Ca^{2+} transients (Figures 3 and 4) and alters mitochondrial membrane potential (Figure 2). Our results also show that crotamine can induce cell death by activating the executive enzyme caspase (Supporting Information S2).[23]

Accumulation of crotamine in actively proliferating cells has already been documented by our group *in vitro*[21] and *in vivo*, using microscopy on tissue samples.[22,23] The use of noninvasive and real-time optical imaging for tracking the whole-body distribution of ip injected fluorescently labeled crotamine (crotamine−Alexa 700), in particular to monitor its accumulation in SC tumors, provides a more complete and straightforward understanding of the *in vivo* localization of this molecule. Although 2D-FRI is not adapted to the study of B16F10 tumors in mice, due to the heavy absorbance of melanine produced by these cells (Figures 5A and 5B), a histological analysis of B16F10 sections confirmed the tumor targeting potential of Cy3−crotamine (Figure 5C). HE staining showed the typical morphology of melanoma cells (Figure 5D). On the other hand, Alexa 700−crotamine fluorescence was observed by 2D-FRI in the murine breast tumor model TS/A-pc SC tumors as early as 15 min after ip injection (Figure 6), and this signal lasted for at least 5 h (Figure 6, Supporting Information S4 and Supporting Information S5). The tumor-targeting properties of crotamine were also demonstrated on disseminated nodules located in the peritoneal cavity, using bioluminescent TS/A-pc tumor cells (TS/A-pc-pGL3) that form a myriad of small nodules after ip injection. An overlap (Figure 7C,F,I) of the bioluminescence of the TS/A-pc-pGL3 tumor nodules (Figure 7A,D,G) and the fluorescence of crotamine−Alexa 700 (Figure 7B,E,H) was observed in these tumor tissues in live animals (Figure 7A−I). This overlap was confirmed after autopsy and exposure of the internal organs directly to the camera (Figure 7J). Moreover, fluorescent microscopy analysis of the TS/A-pc-pGL3 tumor nodule sections showed that crotamine accumulated preferentially in the tumor cells located in the periphery of the tumors (Figure 8).

Based on this evidence, our study clearly shows that crotamine has a pronounced cytotoxic effect on tumor cells *in vitro* and has strong specificity for tumor tissues *in vivo*, demonstrated by the colocalization of crotamine with tumor tissues and cells using a noninvasive real-time optical imaging system. The *in vivo* specificity of crotamine, which was not shown to be affected by its involvement in DNA complex formation,[22] strongly suggests a dual potential role for crotamine: as a prototype to develop a diagnostic marker for cancer and for its use as a therapeutic agent due to its cytotoxic effect on proliferating cells, which could also be enhanced by linking crotamine to other therapeutic molecules or genes. The *in vivo* tumor binding specificity of crotamine and its selective uptake by these tumor cells shown here provide the necessary evidence to justify further *in vivo* studies to evaluate the antitumor efficacy of crotamine in animal models, as it was recently demonstrated by our group.[47] We also intend to evaluate the use of this peptide as a cargo carrier of therapeutic molecules, as already described for other CPPs that lack the *in vivo* tumor targeting specificity of crotamine.[18]

■ ASSOCIATED CONTENT

Ⓢ Supporting Information

Additional figures as described in the text. This material is available free of charge via the Internet at http://pubs.acs.org.

■ AUTHOR INFORMATION

Corresponding Author

*M.A.F.H.: Universidade Federal de São Paulo (UNIFESP), Departamento de Farmacologia, Rua 3 de maio 100 - Ed INFAR, 3rd floor, 04044-020, São Paulo, SP, Brazil; phone, 55-11-5576 4447; fax, 55-11-5576 4499; e-mail, mhayashi@unifesp.br or mirianhayashi@yahoo.com. J.-L.C.: INSERM-UJF U823, Cibles diagnostiques ou thérapeutiques et vectorisation de drogues dans le cancer du poumon, Université Joseph Fourier-Site Santé, Institut Albert Bonniot - BP170, 38042 Grenoble Cedex 9, France; phone, +33 4 76 54 95 53; fax, +33 4 76 54 94 13; e-mail, jean-luc.coll@ujf-grenoble.fr.

Author Contributions

‡These authors contributed equally to this work.

■ ACKNOWLEDGMENTS

This work was supported by Fundação de Amparo à Pesquisa do Estado de São Paulo (FAPESP) and Conselho Nacional de Desenvolvimento Científico e Tecnológico (CNPq). M.A.F.H. was also supported by fellowship from University Joseph Fourier of Grenoble.

■ ABBREVIATIONS USED

CPP, cell penetrating peptide; Cy3−crotamine, Cy3-conjugated crotamine; crotamine−Alexa 700, Alexa 700-conjugated crotamine; JC-1, 5,5′,6,6′-tetrachloro-1,1′-3,3′-tetraethylbenzimidazolcarbocyanine iodide; DIC, differential interference contrast; FBS, fetal bovine serum; ER, endoplasmic reticulum; ROI, regions of interest; SERCA, sarco/endoplasmic reticulum Ca^{2+}-ATPase; TS/A-pc-pGL3, TS/A-pc cells containing luciferase vector; A.U., arbitrary unit

■ REFERENCES

(1) Nguyen, Q. T.; Olson, E. S.; Aguilera, T. A.; Jiang, T.; Scadeng, M.; Ellies, L. G.; Tsien, R. Y. Surgery with molecular fluorescence imaging using activatable cell-penetrating peptides decreases residual cancer and improves survival. *Proc. Natl. Acad. Sci. U.S.A.* **2010**, *107*, 4317−4322.

(2) Albrecht, H.; Radosevich, J. A.; Babich, M. Fundamentals of antibody-related therapy and diagnostics. *Drugs Today* **2009**, *45*, 199−211.
(3) Koopmans, K. P.; Neels, O. N.; Kema, I. P.; Elsinga, P. H.; Links, T. P.; de Vries, E. G.; Links, T. P.; de Vries, E. G.; Jager, P. L. Molecular imaging in neuroendocrine tumors: molecular uptake mechanisms and clinical results. *Crit. Rev. Oncol. Hematol.* **2009**, *71*, 199−213.
(4) Eberle, A. N.; Mild, G. Receptor-mediated tumor targeting with radiopeptides. Part 1. General principles and methods. *J. Recept. Signal Transduction Res.* **2009**, *29*, 1−37.
(5) Griggs, J.; Zinkewich-Peotti, K. The state of the art: immune-mediated mechanisms of monoclonal antibodies in cancer therapy. *Br. J. Cancer* **2009**, *101*, 1807−1812.
(6) Frank, R. T.; Edmiston, M.; Kendall, S. E.; Najbauer, J.; Cheung, C. W.; Kassa, T.; Metz, M. Z.; Kim, S. U.; Glackin, C. A.; Wu, A. M.; Yazaki, P. J.; Aboody, K. S. Neural stem cells as a novel platform for tumor-specific delivery of therapeutic antibodies. *PLoS One* **2009**, *4*, e8314.
(7) Ko, E. C.; Wang, X.; Ferrone, S. Immunotherapy of malignant diseases. Challenges and strategies. *Int. Arch. Allergy Immunol.* **2003**, *132*, 294−309.
(8) Ghasemi, Y.; Peymani, P.; Afifi, S. Quantum dot: magic nanoparticle for imaging, detection and targeting. *Acta Biomed.* **2009**, *80*, 156−165.
(9) Ting, G.; Chang, C. H.; Wang, H. E. Cancer nanotargeted radiopharmaceuticals for tumor imaging and therapy. *Anticancer Res.* **2009**, *29*, 4107−4118.
(10) Jin, Z. H.; Josserand, V.; Foillard, S.; Boturyn, D.; Dumy, P.; Favrot, M. C.; Dumy, P.; Coll, J. L. *In vivo* noninvasive optical imaging of receptor-mediated RGD internalization using self-quenched Cy5-labeled RAFT-c(-RGDfK-)(4). *Mol. Imaging* **2007**, *6*, 43−55.
(11) Foillard, S.; Sancey, L.; Coll, J. L.; Boturyn, D.; Dumy, P. Targeted delivery of activatable fluorescent pro-apoptotic peptide into live cells. *Org. Biomol. Chem.* **2009**, *7*, 221−224.
(12) Sugahara, K. N.; Teesalu, T.; Karmali, P. P.; Kotamraju, V. R.; Agemy, L.; Greenwald, D. R.; Ruoslahti, E. Coadministration of a tumor-penetrating peptide enhances the efficacy of cancer drugs. *Science* **2010**, *328*, 1031−1035.
(13) Vivès, E.; Richard, J. P.; Rispal, C.; Lebleu, B. TAT peptide internalization: seeking the mechanism of entry. *Curr. Protein Pept. Sci.* **2003**, *4*, 125−132.
(14) Kerkis, A.; Hayashi, M. A.; Yamane, T.; Kerkis, I. Properties of cell penetrating peptides (CPPs). *IUBMB Life* **2006**, *58*, 7−13.
(15) Chugh, A.; Eudes, F.; Shim, Y. S. Cell-penetrating peptides: Nanocarrier for macromolecule delivery in living cells. *IUBMB Life* **2010**, *62*, 183−193.
(16) Harada, H.; Kizaka-Kondoh, S.; Hiraoka, M. Antitumor protein therapy; application of the protein transduction domain to the development of a protein drug for cancer treatment. *Breast Cancer* **2006**, *13*, 16−26.
(17) Lee, J. Y.; Choi, Y. S.; Suh, J. S.; Kwon, Y. M.; Yang, V. C.; Lee, S. J.; Chung, C. P.; Park, Y. G. Cell-penetrating chitosan/doxorubicin/TAT conjugates for efficient cancer therapy. *Int. J. Cancer* **2010**, 2470−2480, DOI: 10.1002/ijc.25578.
(18) Sarko, D.; Beijer, B.; Garcia Boy, R.; Nothelfer, E. M.; Leotta, K.; Eisenhut, M.; Altmann, A.; Haberkorn, U.; Mier, W. The pharmacokinetics of cell-penetrating peptides. *Mol. Pharmaceutics* **2010**, *7*, 2224−2231.
(19) Aguilera, T. A.; Olson, E. S.; Timmers, M. M.; Jiang, T.; Tsien, R. Y. Systemic *in vivo* distribution of activatable cell penetrating peptides is superior to that of cell penetrating peptides. *Integr. Biol.* **2009**, *1*, 371−381.
(20) Olson, E. S.; Aguilera, T. A.; Jiang, T.; Ellies, L. G.; Nguyen, Q. T.; Wong, E. H.; Gross, L. A.; Tsien, R. Y. *In vivo* characterization of activatable cell penetrating peptides for targeting protease activity in cancer. *Integr. Biol.* **2009**, *1*, 382−393.
(21) Kerkis, A.; Kerkis, I.; Rádis-Baptista, G.; Oliveira, E. B.; Vianna-Morgante, A. M.; Pereira, L. V.; Yamane, T. Crotamine is a novel cell-penetrating protein from the venom of rattlesnake *Crotalus durissus terrificus*. *FASEB J.* **2004**, *18*, 1407−1409.
(22) Nascimento, F. D.; Hayashi, M. A.; Kerkis, A.; Oliveira, V.; Oliveira, E. B.; Rádis-Baptista, G.; Nader, H. B.; Yamane, T.; Tersariol, I. L.; Kerkis, I. Crotamine mediates gene delivery into cells through the binding to heparan sulfate proteoglycans. *J. Biol. Chem.* **2007**, *282*, 21349−21360.
(23) Hayashi, M. A.; Nascimento, F. D.; Kerkis, A.; Oliveira, V.; Oliveira, E. B.; Pereira, A.; Rádis-Baptista, G.; Nader, H. B.; Yamane, T.; Kerkis, I.; Tersariol, I. L. Cytotoxic effects of crotamine are mediated through lysosomal membrane permeabilization. *Toxicon* **2008**, *52*, 508−517.
(24) Lemasters, J. J.; Theruvath, T. P.; Zhong, Z.; Nieminen, A. L. Mitochondrial calcium and the permeability transition in cell death. *Biochim. Biophys. Acta* **2009**, *1787*, 1395−1401.
(25) Smaili, S.; Hirata, H.; Ureshino, R.; Monteforte, P. T.; Morales, A. P.; Muler, M. L.; Terashima, J.; Oseki, K.; Rosenstock, T. R.; Lopes, G. S.; Bincoletto, C. Calcium and cell death signaling in neurodegeneration and aging. *An. Acad. Bras. Cienc.* **2009**, *81*, 467−475.
(26) Sancey, L.; Dufort, S.; Josserand, V.; Keramidas, M.; Righini, C.; Rome, C.; Faure, A. C.; Foillard, S.; Roux, S.; Boturyn, D.; Tillement, O.; Koenig, A.; Boutet, J.; Rizo, P.; Dumy, P.; Coll, J. L. Drug development in oncology assisted by noninvasive optical imaging. *Int. J. Pharm.* **2009**, *379*, 309−316.
(27) Morris, M. C.; Depollier, J.; Mery, J.; Heitz, F.; Divita, G. A peptide carrier for the delivery of biologically active proteins into mammalian cells. *Nat. Biotechnol.* **2001**, *19*, 1173−1176.
(28) Boisseau, S.; Mabrouk, K.; Ram, N.; Garmy, N.; Collin, V.; Tadmouri, A.; Mikati, M.; Sabatier, J. M.; Ronjat, M.; Fantini, J.; De Waard, M. Cell penetration properties of maurocalcine, a natural venom peptide active on the intracellular ryanodine receptor. *Biochim. Biophys. Acta* **2006**, *1758*, 308−319.
(29) Bratosin, D.; Mitrofan, L.; Palii, C.; Estaquier, J.; Montreuil, J. Novel fluorescence assay using calcein-AM for the determination of human erythrocyte viability and aging. *Cytometry, Part A* **2005**, *66*, 78−84.
(30) Guse, A. H.; Roth, E.; Emmrich, F. Intracellular Ca^{2+} pools in Jurkat T-lymphocytes. *Biochem. J.* **1993**, *291*, 447−451.
(31) Giles, A. R. Guidelines for the use of animals in biomedical research. *Thromb. Haemostasis* **1987**, *58*, 1078−1084.
(32) Josserand, V.; Texier-Nogues, I.; Huber, P.; Favrot, M. C.; Coll, J. L. Non-invasive in vivo optical imaging of the lacZ and luc gene expression in mice. *Gene Ther.* **2007**, *14*, 1587−1593.
(33) Salvioli, S.; Ardizzoni, A.; Franceschi, C.; Cossarizza, A. JC-1, but not DiOC6(3) or rhodamine 123, is a reliable fluorescent probe to assess delta psi changes in intact cells: implications for studies on mitochondrial functionality during apoptosis. *FEBS Lett.* **1997**, *411*, 77−82.
(34) Bhola, P. D.; Mattheyses, A. L.; Simon, S. M. Spatial and temporal dynamics of mitochondrial membrane permeability waves during apoptosis. *Biophys. J.* **2009**, *97*, 2222−2231.
(35) Keramidas, M.; Josserand, V.; Righini, C. A.; Wenk, C.; Faure, C.; Coll, J. L. Intraoperative near-infrared image-guided surgery for peritoneal carcinomatosis in a preclinical experimental model. *Br. J. Surg.* **2010**, *97*, 737−743.
(36) Boni-Mitake, M.; Costa, H.; Vassilieff, V. S.; Rogero, J. R. Distribution of (125)I-labeled crotamine in mice tissues. *Toxicon* **2006**, *48*, 550−555.
(37) Pinton, P.; Giorgi, C.; Siviero, R.; Zecchini, E.; Rizzuto, R. Calcium and apoptosis: ER-mitochondria Ca2+ transfer in the control of apoptosis. *Oncogene* **2008**, *27*, 6407−6418.
(38) Gupta, S. Molecular steps of death receptor and mitochondrial pathways of apoptosis. *Life Sci.* **2001**, *69*, 2957−2964.
(39) Brenner, D.; Mak, T. W. Mitochondrial cell death effectors. *Curr. Opin. Cell Biol.* **2009**, *21*, 871−877.
(40) Giorgi, C.; Romagnoli, A.; Pinton, P.; Rizzuto, R. Ca^{2+} signaling, mitochondria and cell death. *Curr. Mol. Med.* **2008**, *8*, 119−130.

(41) Gonzalez, D.; Espino, J.; Bejarano, I.; Lopez, J. J.; Rodriguez, A. B.; Pariente, J. A. Caspase-3 and −9 are activated in human myeloid HL-60 cells by calcium signal. *Mol. Cell. Biochem.* **2010**, *333*, 151−157.
(42) Yodozawa, S.; Speake, T.; Elliott, A. Intracellular alkalinization mobilizes calcium from agonist-sensitive pools in rat lacrimal acinar cells. *J. Physiol.* **1997**, *499*, 601−611.
(43) Luzio, J. P.; Rous, B. A.; Bright, N. A.; Pryor, P. R.; Mullock, B. M.; Piper, R. C. Lysosome-endosome fusion and lysosome biogenesis. *J. Cell Sci.* **2000**, *113*, 1515−1524.
(44) Zhu, M. X.; Ma, J.; Parrington, J.; Galione, A.; Evans, A. M. TPCs: Endolysosomal channels for Ca2+ mobilization from acidic organelles triggered by NAADP. *FEBS Lett.* **2010**, *584*, 1966−1974.
(45) Palm-Apergi, C.; Lorents, A.; Padari, K.; Pooga, M.; Hallbrink, M. The membrane repair response masks membrane disturbances caused by cell-penetrating peptide uptake. *FASEB J.* **2009**, *23*, 214−223.
(46) Calcraft, P. J.; Ruas, M.; Pan, Z.; Cheng, X.; Arredouani, A.; Hao, X.; Tang, J.; Rietdorf, K.; Teboul, L.; Chuang, K. T.; Lin, P.; Xiao, R.; Wang, C.; Zhu, Y.; Lin, Y.; Wyatt, C. N.; Parrington, J.; Ma, J.; Evans, A. M.; Galione, A.; Zhu, M. X. NAADP mobilizes calcium from acidic organelles through two-pore channels. *Nature* **2009**, *459*, 596−600.
(47) Pereira, A.; Kerkis, A.; Hayashi, M. A.; Pereira, A. S.; Silva, F. S.; Oliveira, E. B.; Prieto da Silva, A. R.; Yamane, T.; Rádis-Baptista, G.; Kerkis, I. Crotamine toxicity and efficacy in mouse models of melanoma. *Expert Opin. Invest. Drugs* **2011**, *20*, 1189−200.